INSTITUTE FOR RESEARCH AND COMMUNITY SERVICES UPN "VETERAN" YOGYAKARTA

Journal TECHNO

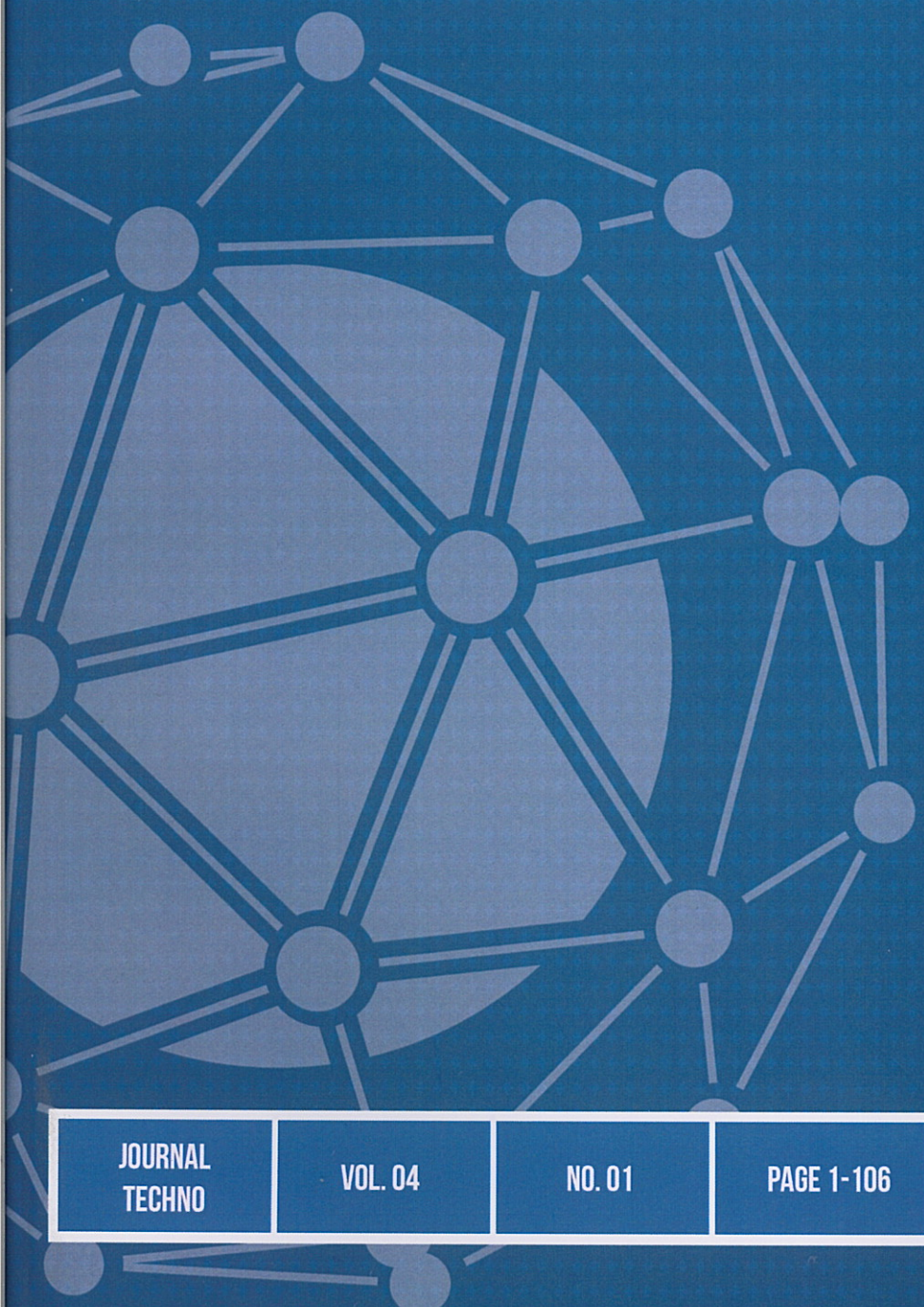

JOURNAL TECHNO	VOL. 04	NO. 01	PAGE 1-106	YOGYAKARTA AUGUST 2018	ISSN 2461-1484

Journal Techno

Editorial Office

Institute for Research and Community Services
Universitas Pembangunan Nasional "Veteran" Yogyakarta
Jl. SWK 104 (Lingkar Utara) Condongcatur, Sleman-Yogyakarta 55283
Phone (62 274) 486733, Fax. (62 274) 486188, email: lppm@upnyk.ac.id

Journal Techno
ISSN : 2461-1484
Vol. 4 No. 1 August 2018

Table of Content

LOCATION PREDICTION AND REDUCTION OF SCALING RATE IN GEOTHERMAL WELLS

Bambang Bintarto, Dewi Asmorowati, Allen H Lukmana
UPN Petroleum Engineering Lecturer

Abstract

Scaling is a common problem that occurs in geothermal wells, particularly wells dominance of water as occurs in several wells in Mount salak awibengkok studied in this thesis. Scale formed on the installation of a geothermal well production can cause a decrease in production wells, it can even lead to cessation of production. Therefore, prevention and handling of scaling issues is very important to be attention.

Scale can be formed due to the chemical reaction by mixing a geothermal fluid with other geothermal fluid is different compositions, or also can be caused by changes in fluid properties due to changes in pressure and temperature cause changes in saturation of the substances making up the geothermal fluid. Substances making up the geothermal fluid will experience a change in saturation due to reactions that occur in the process of evaporation. The point of particular pressure and temperature conditions where the geothermal fluid evaporation is taking place, or start a phase change from one phase into two phases, commonly referred to as Flash Point. In these conditions the substances in excess of its saturation point will have precipitation. By knowing the location of the depth of the steam point or flash point, the geothermal fluid can be estimated where the scaling is the first time this has happened.

The location of the depth of the flash point can be determined by calculating the pressure drop from the well head to the bottom of the well to achieve the conditions of fluid saturation temperature, that is the temperature where the flow is taking place in two phases. For example, there are Beggs & Brill method, Horrison-freeston method, and the Lockhart-Martinelli method. At this time studies used correlation is the correlation Beggs & Brill, which in previous studies considered the most valid.

***Keywords**: scaling, location, formation of scaling, thickness of scaling.*

I. INTRODUCTION

The method used in this study is the application of the silica saturation index (SSI) parameter which is calculated based on the data of the fluid chemical composition, temperature, and pH in the separator and flasher. This SSI parameter compares the concentration of silica in solution with the solubility of amorphous silica in the same conditions.

SSI> 1, fluid in supersaturated conditions and scaling is possible.

SSI = 1, the fluid is in saturated condition.

SSI <1, the fluid is undersaturated, so there is no precipitation.

$$SSI = \frac{Q(t_1,m)}{[s(T,m)(1-x_2)]} \quad (1)$$

$Q(t_1,m)$ = Quartz solubility at reservoir temperature (t1) and salinity m

$s(T,m)$ = Amorphous solubility at flashing and salinity temperatures m

$x2$ = Quality of steam flashing

Silica scaling formation increases with decreasing temperature and increasing pH due to flashing. the rate of silica scaling thickening that occurs in the production

pipe and the estimated time of silica scaling can clog the pipe up to 25% of the original pipe diameter can be calculated by the following equation.

$$\dot{S}_t = \frac{Q(t_1,m)-s(T,m)}{1743\ x\ \rho_{silika}} x\ 365 \quad (2)$$

$$t_{25\%} = \frac{D}{4\ x\ \dot{S}_t} \quad (3)$$

With

S t = Silica scaling (inch / year) rate

$\rho silica$ = Density of silica = 43,442 g / in3

Q ($t1$, m) = quartz solubility at reservoir temperature (t1) and salinity m

s (T, m) = amorphous solubility at the flashing temperature and salinity m

D = pipe diameter (inch)

Silica scaling on fluid injection pathways is controlled by the chemical and thermodynamic properties of amorphous silica. The heat transfer process that takes place is exothermic (the system releases heat to the environment) because the temperature of the fluid is higher than the temperature of the environment. The heat transfer process causes the temperature distribution of the fluid as it flows along the pipeline.

The chemical properties of amorphous silica which directly affect the formation of scaling are saturation solubility (saturation) as a function of temperature. The presence of fluid temperature distribution during the production or injection process causes the amorphous silica saturated solubility to decrease along the pipeline.

Fluid Temperature Distribution Analysis

To analyze the fluid temperature distribution along the pipeline, the first thing to do is to do an energy analysis on the system. In conducting this energy analysis, researchers divided the volume control into several parts in the form of cells.

Amorph Silika (ppm)= - 6E - $05T^3 + 0.0333T^2$ - 0.0327T + 88.773 (4)

The above equation is an equation formed from the amorphous silica solubility graph (Figure 1). The next step is to compare the dissolved fraction in the brine to the actual conditions with the saturated silica solubility calculated for each cell. If the conditions for the precipitation reaction are fulfilled (the dissolved silica fraction > saturated solubility in the same conditions), the amount of the precipitation reaction that occurs can be calculated by entering the Tn value and the pH of brine to the reaction equation, namely:

$$Rx\ rate\ \left(\frac{mol}{m^2 s}\right) = -10^{-5.7}.10^{\left(-\frac{26.9}{2.303RT}\right)} + 10^{(-13.7+1.9(pH)}.10^{\left(-8.15.\frac{pH}{2.303RT}\right)} \quad (5)$$

Scaling Thickening Rate The magnitude of the scaling thickening rate can be found by assuming that the rate of change in the volume of scaling formed is proportional to the mass rate of silica which settles with the multiplier, namely the silica mass itself..

$$\frac{dV_{sil}}{dt} = \frac{d_m}{dt} \cdot \frac{1}{\rho_{sil}} \quad (6)$$

Scaling thickening can be expressed in forms :

$$\frac{d_\theta}{dt}\left[A - B\theta + \frac{C_t}{\rho_{sil}}\right] = \frac{CR_{in}}{\rho_{sil}} \cdot \frac{C_\theta}{\rho_{sil}} \quad (7)$$

where :

A = 2□R_{in}L

B = 2□L

C = M_{total}.R_x.MR.2□□L

Multiple Linear Regression Analysis

Multiple Linear Regression Analysis is a multivariate technique that is used to estimate the relationship between one dependent metric variable and one set of metric or nonmetric independent variables. With multiple regression analysis researchers can estimate and or predict the average value (population) of a dependent variable based on two or more independent variables. Regression analysis will produce an equation / regression model.

This regression equation / model will be used in the analysis of the relationship between the concentration of Silica Ion and the speed of the reaction of Scale Silica formation in the Geothermal Reservoir.

As an example of regression analysis, a researcher suspects that the level of sales of certain products is influenced by the amount of advertising funds, the number of salesmen deployed and the number of outlets scattered in each place. For the purposes of this study, researchers can take advantage of multiple regression analysis by placing the level of sales as the metric dependent variable and the other three variables as metric independent variables. Researchers will obtain a regression model that can be used to explain and predict the level of sales variance that is influenced by the three independent variables.

The basic model of this multiple regression analysis technique is as follows:

$$\hat{Y} = \beta_0 + \beta_1 X_1 + \beta_2 X_2 + \beta_3 X_3 + \cdots + \beta_i X_i \quad (8)$$

$\hat{Y}$: Predict the value of the dependent variable

β_0 : Constants (intercept)

β_i : Regression weight (coefficient) for the independent variable i

X_i : The independent variable i

Numerical analysis modeling

The numerical analysis used in this study is related to the computation (estimation) solution of differential equations, both ordinary differential equations and partial differential equations. The partial differential equation is solved by first discrete the equation, bringing it into finite-dimensional subspace. This can be done with the finite element method, finite difference method. The theoretical justification of the method will be used involving the theorem from functional analysis to reduce the problem to the solution of algebraic equations.

The partial differential equation is solved by first discrete the equation, bringing it into finite-dimensional subspace. This can be done with the finite element method, finite difference method. The theoretical justification of the method will be used involving the theorem from functional analysis to reduce the problem to the solution of algebraic equations.

Partial differential equation (PDE) is an equation that involves the degree of change with respect to a continuous variable. Rigid body position is determined by six parameters [1], but the fluid configuration is given by the continuous distribution of several parameters, such as temperature, pressure, and so on. The dynamics for a rigid body take place in a finite dimensional configuration space; fluid dynamics occur in infinite dimension configuration spaces. This difference usually makes PDE harder to solve than ordinary differential equations (ODE), but here again, there will be a simple solution for linear problems. The classic domain where PDE is used includes acoustics, fluid

dynamics, electrodynamics, and heat transfer.

A partial differential equation (PDE) for this function is an equation of form :

$$f\left(x1, \ldots, xn, u, \frac{\partial u}{\partial x1}, \ldots, \frac{\partial u}{\partial xn}, \frac{\partial^2 u}{\partial x1 \partial x1}, \ldots, \frac{\partial^2 u}{\partial x1 \partial xn}, \ldots\right) = 0 \quad (8)$$

If f is a linear function of u and its derivative, then PDE is called linear. Common examples of linear PDE include heat equations, which are wave equations, Laplace equations, Helmholtz equations, Klein-Gordon equations, and Poisson equations.

II. ESTABLISHMENT OF SCALE

Generally the scale formed in a geothermal well is calcium cabonate, with calcium and carbonate as a component; Amorphous Silica, which is formed from silica, and other mineral deposits.

2.1 The occurrence of scaling in geothermal wells

Changes in the fluid phase from the liquid phase due to changes in pressure and temperature trigger a decrease in fluid pH. The reaction that occurs in the fluid when the phase change is as follows,

$H_2CO_3 \rightarrow 2H^+ + CO_3^{2-}$
$H_2S \rightarrow 2H + S^{2-}$
$Ca^{2+} + CO_3^{2-} \rightarrow CaCO_3\downarrow$
$Me^{2+} + S^{2-} \rightarrow MeS\downarrow$
(Me = Fe, Zn, Cu, dll)

When it reaches the flash point condition, Carbonic Acid will break down into Hydrogen ions that bind to Oxygen to form water vapor, and carbonate ions that bind to calcium ions to form calcium carbonate which then settles and is cemented. Under these conditions, Hydrogen sulfide will break down into hydrogen and sulfide ions which when bound to metal ions form metal deposits (Figure 2.1). The sediments will then be cemented and form a crust on the well wall and cause constriction or blockage of the well.

2.2 Scaling type

Based on the location of the formation of scaling is divided into 3 types: the first type is the scaling that occurs in the wellbore, which is discussed in this final project; the second type is scaling that occurs on surface equipment. Generally the type of sediment is amorphous silica deposits, calcium carbonate and silica. Sediments occur in equipment with a low fluid flow velocity, for example separators and tanks; the third type is scaling that occurs in injection wells, the type of sediment in this type is amorphous silica deposits.

2.3 Scaling countermeasures method

There are four important principles in dealing with scaling problems:

1. Limiting the concentration of minerals causing scaling by preventing the entry of these minerals in the geothermal system.
2. Maintain acidity to prevent scale formation, especially calcite.
3. Making a production design that allows no scale.
4. Use chemicals to prevent scale deposition reactions.

III. PROPERTIES GEOTHERMAL FLUID

The main fluid of geothermal is water, therefore the knowledge needed is about the properties of water fluid, especially its relation to temperature and pressure. Calculation of fluid properties can be approximated by using correlation. The properties of the fluid needed by its values include saturation temperature, viscosity, density, and enthalpy which are approximated by the correlation of the Tortike polynomial equation and Farouq Ali.

3.1 Saturation temperature

The price of the saturation temperature for a given pressure can be seen in the steam table or can be approximated by a polynomial equation. The polynomial equation only applies to certain pressure ranges, namely 0.611 kPa ≤ P ≤ 22.12 Mpa. The equation is as follows:

$$T_s = 280.034 + 14.0856 \ln P + 1.38075 (\ln P)^2 - 0.101806 (\ln P)^3 + 0.019017 (\ln P)^4 \quad (3.1)$$

Where, Ts is the saturation temperature, K (Kelvin); P is pressure, kPa (kilo Pascal)

3.2 Density

The amount of fluid density at saturation conditions can be obtained by the polynomial equation as follows :

$$\rho_l = 3786.31 - 37.2487\ T + 0.196246\ T^2 - 5.04708 \times 10^{-4}\ T^3 + 6.29368 \times 10^{-7}\ T^4 - 3.0848 \times 10^{-9}\ T^5 \quad (3.2)$$

$$\rho_g = Exp\ [\ -93.7072 + 0.833941\ T - 0.00320809\ T^2 + 6.57652 \times 10^{-6}\ T^3 - 6.93747 \times 10^{-9}\ T^4 + 2.97203 \times 10^{-12}\ T^5\ ] \quad (3.3)$$

Where, ρl is the fluid density, kg/m3; ρg is the gas density, kg/m3; T is the temperature, K. Equation (3.2) applies to temperatures of : 273.15 ≤ T ≤ 640 K. while equation (3.3) applies to temperatures: 273.15 ≤ T ≤ 645 K.

3.3 Enthalpy

Enthalpy is the sum of the inner energy and energy produced by pressure work. Inner energy is the amount of heat the mass of mass contained in a material. Steam enthalpy is the amount of enthalpy of water at saturation conditions plus boiling heat or latent heat. The amount of enthalpy can be determined by the following polynomial equation,

$$h_f = 23665.2 - 366.232\ T + 2.26952\ T^2 - 0.00730365\ T^3 + 1.30241 \times 10^{-5} T^4 - 1.22103 \times 10^{-8}\ T^5 + 4.70878 \times 10^{-12}\ T^6 \quad (3.4)$$

$$h_g = -22026.9 + 365.317\ T - 2.25837\ T^2 + 0.00737420\ T^3 - 1.33437 \times 10^{-5}\ T^4 + 1.26913 \times 10^{-8} T^5 - 4.9688 \times 10^{-12}\ T^6 \quad (3.5)$$

Where, hf is liquid enthalpy (kJ / kg); hg is enthalpy vapor (kJ / kg), T is temperature (oK). Equation (3.4) applies to temperatures of 273.15 ≤ T ≤ 645 K. while equation (3.5) applies to temperatures of 273.15 ≤ T ≤ 640 K.

3.4 Viskosity

viscosity is a fluid property that shows the amount of fluid aversion to flow. There are two types of viscosity, dynamic viscosity (μ) and kinematic viscosity (v). Dynamic viscosity is strongly influenced

by temperature but is very little affected by pressure.

the magnitude of fluid dynamic viscosity at saturation conditions can be determined by the polynomial equation as follows,

$$\mu_l = -0.0123274 + 27.1038\,T^{-1} - 23527.5\,T^{-2} + 1.0425x10^{7}\,T^{-3} - 2.17342x10^{9}\,T^{-4} + 1.86935x\,10^{11}\,T^{-5} \quad (3.6)$$

$$\mu_g = -5.46807x10^{-4} + 6.8949x10^{-6}\,T - 3.39999\,x10^{-8}\,T^{2} + 8.29842x10^{-11}\,T^{3} - 9.9706x10^{-14}\,T^{4} + 4.71914x10^{-17}T^{5} \quad (3.7)$$

μl is the viscosity of the liquid (kg / m.s); μg is steam viscosity (kg / m.s); T is temperature (oK).
Equation (3.6) applies to temperatures of $273.15 \leq T \leq 640$ K. While equation (3.7) applies to $273.15 \leq T \leq 645$ K.

3.5 Surface Voltage

Surface tension is the energy of broad unity needed for each increase in fluid surface area (usually expressed in a style of long unity). Surface tension depends on elements dissolved in water and fluid temperature, while the influence of pressure is too small. The price of surface tension for water at a certain temperature can be obtained from the table of the physical properties of the fluid or with the equation :

$$\sigma_L = 0.2358\ x\ \left(\frac{374-T}{647.15}\right)^{1.256}\left(1 - 0.625\left(\frac{374-T}{647.15}\right)\right) \quad (3.8)$$

σL is surface tension (N / m); T temperature (oC). Equation (3.8) applies to temperatures of $273.16 \leq T \leq 647.15$ K.

3.6 Quality of steam

The quality of steam or dryness (x) is defined as the ratio between the rate of steam phase and the total mass rate. The quality of steam in a mixture of vapors at saturation pressure and temperature can be determined if the enthalpy price of the mixture is known. The quality of steam or dryness can be calculated using the equation,

$$x = \frac{h-hf}{hg-hf} \quad (3.9)$$

h is enthalpy fluid (water-vapor mixture) in kJ / kg.

IV. TWO PHASE FLUID FLOWS

Knowledge of the type of flow and the ratio of the amount of water vapor is very important in studying the behavior of fluid flow in the pipe, especially to study the pressure drop in the pipe.

4.1 Flow Pattern

There are several factors that determine the condition of fluid flow that occurs in geothermal systems including the ratio (comparison) between water vapor and water, and the diameter of the pipe used. Steam and water have different flow velocities, so there is a slip between the two phase fluids. When the fluid flows up there is a pressure drop whose magnitude is determined by friction on the pipe wall, acceleration, and gravity. As pressure drops, bubbles begin to form and a two-phase flow pattern is formed.

4.2 *Beggs & Brill correlation*

Calculation of pressure on vertical pipes can be approximated by various

correlation equations, including Beggs & Brill correlation, Horrison-freeston correlation, Duns & Ros, Hagedorn & Brown correlation, and Lockhart-Martinelli1 correlation). Among these correlations based on existing tests, the correlation between Beggs & Brill is considered the most accurate. Therefore, in this study, the Beggs & Brill correlation was used.

Liquid velocity number

$$Nlv = Vsl\left(\frac{\rho l}{g\,\sigma}\right)^{1/4} \quad (4.1)$$

Froude Number

$$N\,fr = \frac{Vm^2}{g\,dh} \quad (4.2)$$

Homogeneous Liquid Holdup

$$\lambda = \frac{Vsl}{Vm} \quad (4.3)$$

$$Vsl = \frac{W}{A} \quad (4.4)$$

$$Vsg = \frac{S}{A} \quad (4.5)$$

$$Vm = Vsl + Vsg \quad (4.6)$$

Vsl is the superficial velocity of water (m / s); Vsg is the superficial velocity of water vapor (m / s); Vm is the two phase fluid velocity (m / s); W is the mass flow rate of water and steam (kg / s).

Beggs & Brill divides fluid flow patterns on the following three flow patterns,

1. Segregated flow pattern, if:

$Nfr < L_1$

2. Distributed flow pattern, if:

$Nfr > L_1$ *dan* $Nfr > L_2$

3. Intermittent flow pattern, if:

$L_1 < Nfr < L_2$

$$L1 = Exp\,(-4.62 - 3.757\,K - 0.481\,K^2 - 0.207\,K^3) \quad (4.7)$$

$$L2 = Exp\,(1.061 - 4.602\,K - 1.609\,K^2 - 0.179\,K^3 + 0.635x10^{-3}\,K^5) \quad (4.8)$$

$$K = Ln\,(\lambda) \quad (4.9)$$

After that, liquid holdup (Hl) can be calculated from the horizontal liquid holdup Hl (0) and inclination factor, C.

$$H_l = H_l(0)\ \Psi \quad (4.10)$$

$$\Psi = 1 + C\,(sin(1.8\,\theta) - 0.333\,sin\,(1.8\,\theta)) \quad (4.11)$$

For vertical flow, θ = 90°, equation (4.11) becomes:

$$\Psi = 1 + 0.3\,C \quad (4.12)$$

$$H_l(0) = \frac{A\,\lambda^B}{Nfr^D} \quad (4.13)$$

$$C = (1-\lambda_L)\,ln(\alpha\,\lambda_L^{\,e}\,N_{lv}^{\,f}\,N_{fr}^{\,g}) \quad (4.14)$$

For Segregated flow patterns,
A= 0.98; B= 0.4846; D= 0.0868
α= 0.011; e= -3.768; f= 3.539; g= -1.614

For Intermittent flow,
A= 0.845; B= 0.5351; D= 0.0173
α= 2.96; e= 0.305; f= -0.4473; g= 0.0978

For Distributed flow,
A= 1.065; B= 0.5824; D= 0.0609
(C= 0)

4.3 Pressure gradients due to friction

Pressure gradients caused by friction are defined by Beggs & Brill as follows,

$$\left(\frac{dp}{dz}\right)_f = f_{tp}\rho_n \frac{V_m^2}{2\,dh} \qquad (4.15)$$

Where ftp is a friction factor for two-phase flow, which does not depend on the angle of inclination, but depends on in-situ (or actual) and liquid holdup as follows,

$$f_{tp} = f_n\, e^S \qquad (4.16)$$

$$S = \frac{[ln(y)]}{\{-0.0523+3.1821\ln(y)-0.8725[\ln(y)]^2+0.8725[\ln(y)]^3\}} \qquad (4.17)$$

$$y = \frac{\lambda}{H_l^2} \qquad (4.18)$$

For 1 <y <1.2 equation (4.17) to be infinite, then S is defined again as:

$$S = ln(2.2y - 1.2) \qquad (4.19)$$

While friction factor (fn) is evaluated as friction in a single phase using the Colebrook equation, with its Reynold number defined as follows :

$$N_{Re} = \frac{[\rho_l\lambda + \rho_g(1-\lambda)]\,V_m dh}{\mu_l\lambda + \mu_g(1-\lambda)} \qquad (4.20)$$

The equation for calculating homogeneous friction factors (Colebrook & White, 1939):

$$f_n = \left[\frac{1}{1.74-2log\left(\frac{2\varepsilon}{d}+\frac{18.7}{N_{Re}\sqrt{f_a}}\right)}\right]^2 \qquad (4.21)$$

ε is the absolute roughness of the pipe, if no data is available it can be assumed that the price is 0.0006 ft or 0.00018288 m. d is the diameter of the pipe, ft or meter.

The above equation is an implicit equation, so to find the price of fn must be done by trial and error. For the first iteration, the price of the assumption friction factor (fa) is calculated using the Nikuradse equation (1933) as followss,

$$f_a = \left[\frac{1}{1.74-2log\left(\frac{2\varepsilon}{d}\right)}\right]^2 \qquad (4.22)$$

From the f_a price is used to determine the price of f_n in equation (4.21), until the accuracy is around:

$$\left|\frac{(f_n - f_a)}{f_a}\right| < 0.001 \qquad (4.23)$$

4.4 Pressure gradients due to acceleration

The pressure gradient due to the acceleration of the flow conditions is approximated by the following equation :

$$\left(\frac{dp}{dz}\right)_a = \frac{\rho_s V_m V_{sg}}{P}\left(\frac{dp}{dz}\right)_t \qquad (4.24)$$

4.5 Gradient Pressure due to Potential Energy

The pressure gradient due to changes in height becomes :

$$\left(\frac{dP}{dL}\right)_{el} = \frac{g}{gc}\rho_{tp}\, sin\theta \qquad (4.25)$$

4.6 Total Pressure Gradients

The total pressure gradient is a combination of pressure gradient as the effect of friction, elevation (height), and acceleration (acceleration). The form of the equation is as follows,

$$\frac{\Delta P}{\Delta Z} = \frac{\frac{g\rho_{tp}}{g_c}\sin\theta + \frac{f_{tp}G_m V_m}{2g_c d}}{1 - \frac{\rho_{tp} V_m V_{sg}}{g_c P}} \qquad (4.26)$$

P is the inner pressure (Pa)

4.7 Calculation of Pressure Loss

The following is the procedure performed on Beggs & Brill method in determining pressure loss. The flow chart can be seen in Figure 4.2.

1. Enter initial conditions data (wellhead pressure, mass flow rate, enthalpy and well geometry)
2. Based on the initial pressure of P_1, estimate the price of ΔP.
3. Calculate the average pressure with equation (4.27)

$$P_{ave} = P_1 + \frac{\Delta P}{2} \qquad (4.27)$$

4. Calculate Ts with equation (3.1)
5. Calculating enthalpy of water (hl) and enthalpy vapor (hg) with equations (3.4) and (3.5).
6. Determine the level of steam or dryness (X) using the equation (3.9)
7. calculate the water flow rate (Wp) and water vapor (Sp) at the condition of the mean pressure from dryness data using equations (4.28) and (4.29).

$$S_P = W_P X_P \qquad (4.28)$$

$$W_p = W_{p1}(1 - X_P) \qquad (4.29)$$

8. Calculate the superficial velocity of water (Vsl) and water vapor (Vsg), and mixture (Vm) using equation (4.4), (4.5) and (4.6).
9. Calculate the density of water and water vapor with equations (3.2) and (3.3).
10. Calculate the mass flow rate of water (Gl), water vapor (Gs), and water-vapor mixture using equation (4.30), (4.31), and (4.32)

$$G_l = \rho_l V_{sl} \qquad (4.30)$$

$$G_s = \rho_s V_{sg} \qquad (4.31)$$

$$Gm = Gl + Gs \qquad (4.32)$$

11. Calculates no-slip holdup (λ) using equation (4.3).
12. Calculate Nfr, Viscosity (μm), and surface tension (σ) using equations (4.33), (4.2), (3.6), (3.7), and (3.8).

$$\mu_m = \mu_l \lambda + \mu_g (1-\lambda) \qquad (4.33)$$

13. Calculate Nre, and Nlv using equation (4.20) and (4.1).
14. Calculate L1 and L2 using equation (4.7), and (4.8)
15. Determine the flow pattern based on the values of L1, L2 and Nfr.
16. Calculate vertical liquid holdup (Hl) using equation (4.10).
17. Calculate the two-phase density (ρtp) using equation (4.34).

$$\rho_{tp} = \rho_l H_l + \rho_g (1-H_l) \qquad (4.34)$$

18. Calculate the two-phase friction factor (ftp) using the equation (4.16).
19. Calculate ΔP / ΔZ using equation (4.25).
20. If the ΔP obtained in step 19 is not the same as the estimated value in step 2, then use the ΔP obtained in step 19 as a new assumption in step 2, repeat the calculation until the same or almost the same ΔP is obtained.

V. PRESSURE LOSS SIMULATOR

The simulator used to determine the pressure loss in the wellbore in this study is in the form of an analytical simulator, namely by using a mathematical equation in the form of correlation. In this simulator the Beggs & Brill correlation is used to get a price of pressure, temperature, steam frequency, and enthalpy of evaporation against a certain depth interval. This correlation can be used to explain the pressure loss from the bottom of the well to the wellhead. The fluids used in this correlation are considered pure water or pure water vapor without solids or saline solutions and non-condensable gases. Whereas fluid properties such as density, viscosity, temperature, enthalpy, and surface tension of water and water vapor are approached by the correlation of Tortike & Farouq Ali6) (1989). Some other assumptions used in this simulator include:

1. Inflow only occurs at the bottom of the well, there is no fluid coming in from the well wall.
2. There is no transfer and heat loss as long as the fluid flows in the well.
3. Flow follows Darcy's formula, and reservoir character distribution (permeability, thickness, porosity) is uniform.

5.1 Input and Output

The simulators made in this study are intended to facilitate the calculation of long vertical wells pressure losses and require repeated iterations. The simulator is made in the Macroexcel program with visual basic language.

The data needed to run the simulator is (Figure 5.1):

1. Well geometry: depth and size of casing and liner in meters; and rougness.
2. Pressure of the wellhead (embers).
3. Mass flow rate (kg / s).
4. Enthalpy production (kJ / kg)
5. Hose depth (ft)

The output data from the simulator is in the form of pressure calculation data. The output data is in the form of depth data, namely data (Figure 5.2):

1. Pressure (coals)
2. Dryness (X)
3. Enthalpy (kJ / kg)
4. Flow pattern

By obtaining data on dryness output (X) in depth, it can be known at what depth the fluid phase changes begin to occur. Furthermore, it can be estimated at what depth the scale began to form.

5.2 Alignment Simulator

The simulator that has been made must be validated with field data in order to get the simulator accuracy. Field data used are geothermal wells TM 1-5 data, awibengkok mount salak which has previously been analyzed for the existence of scaling by Hidayatus Sufyan (2009). To obtain alignment with the field data, the modified parameter of the simulator is the lamination friction factor (ε).

5.3 Sensitivity Testing Simulator

After the simulator is considered valid enough to be applied in the field, the simulator is then used to study changes in well behavior for various conditions or sensitivity tests.

Some of the parameters that are changed are: wellhead pressure, casing size, and mass flow rate, which will be affected by changes in the depth of Flash Point.

The pressure of the wellhead tested the difference in effect was 9 coals, 8 coals, 7 coals, and 6 coals; for the casing size, the standard well type and bighole are used; while for the flow rate of the used period 40 kg / s, 50 kg / s, 60 kg / s, 70 kg / s, 80 kg / s, and 100 kg / s.

5.4 Well Case Study

The purpose of making this simulator is to find out the pressure, temperature, dryness of the depth without having to do well testing directly. After being considered quite valid, this simulator will be used to find out well information as mentioned above. The data obtained will then be used to determine optimization recommendations and address the well problem. The wells tested in this study are TM 7-1, TM 7-2, TM, 7-3, TM 7-4, and TM 7-5 wells.

VI. DISCUSSION

To complete the simulator that has been made, it is necessary to synchronize. The parameters that are changed to get alignment with field data are the parameters of rougness (ε) or pipe roughness. From table 6.1, it can be seen that the value of ε to produce the program output that is closest to the condition of the field is the value of 0.00003 m, where the depth of the flash point output of the program is 3625.3 m while the field data is 3629 m. This ε value is still below the assumption ε value for the standard pipe which is 0.00018288 m, this is because when testing the condition of the pipe is not like the initial condition of the pipe.

To get knowledge about the relationship between well parameters, sensitivity testing was carried out on the simulator. The sensitivity tested is the effect of changes in well pressure on the flash point depth, the effect of the combination of well diameter size on the flash point depth, and the effect of changes in the mass flow rate to the flash point depth.

From the results of testing the wellhead pressure parameters (Figure 6.1) shows that the greater the pressure of the wellhead, the more the flash point will be. This is because the greater the pressure, the longer the pressure drops to the saturation pressure.

From the test results for the combination of wellbore size types (Figure 6.2), it is obtained the knowledge that bighole wells produce a deeper flash point depth than standard wells, this is because the larger the size of the wellbore, the smaller the pressure loss due to friction. Standard well combinations are 13 3/8 ', 9 5/8', and 7 ', while for bighole are 20', 13 3/8 ', and 9'.

From the test results on changes in mass flow rate, it was found that the well will be optimal (the biggest flash point depth) at a certain mass flow rate. In this case (Figure 6.3) the optimum mass flow rate is estimated at 60 kg / s.

From the results of field testing, it was obtained information that for the TM 7-1 well there was no flashing inside the wellbore (Figure 6.4), meaning that two-phase flow had occurred since in the reservoir, this gave the possibility of scaling and thickening of scaling per year in the wellbore getting smaller. In the TM 7-2 well, flashing occurs at a depth of 600 meters (Figure 6.5), so that scaling is possible above the depth. In the TM 7-3 well, flashing occurred at a depth of 550 meters (Figure 6.6), so that scaling and thickening of the scaling per year above that depth is possible. In the TM 7-4 well, flashing occurred at a depth of 850 meters (Figure 6.7), so that scaling is possible above the depth. In the TM 7-5 well, flashing occurs at a depth of 850 meters (Figure 6.8) so that scaling is possible above the depth
SAN.

VII. CONCLUSIONS AND RECOMMENDATIONS

7.1 Conclusion

1. The simulator is made using the Macroexcel program with visual basic language, using the Beggs & Brill correlation.
2. The simulators made in the study are valid enough to be used for field testing.
3. After sensitivity testing, the following conclusions are obtained;

a) The greater the pressure of the wellhead, the deeper the depth of the flashing occurs.
b) The bigger the size of the wellbore, the deeper the flash point depth will be.
c) At each well there is an optimum mass flow rate for the deepest flash point.

4. The roughness value of the wellbore cannot be ascertained in this study because the conditions of the well are different from the initial conditions.
5. In the TM 7-1 well there is no flashing in the wellbore, so there is little chance of scaling in the wellbore. Whereas in the wells TM 7-2, TM 7-3, TM 7-4, TM 7-5 flashing occurs in the well which allows scaling in the well.

7.2 Suggestion

1. Improve the simulator by aligning it using other existing simulator results that have been used in the field.
2. Improving the simulator by calculating single-phase flow.
3. Conducting well testing with different wellhead pressures, to get a change in depth of the formation of the scale against changes in wellhead pressure.

VIII. LIST OF NOTATIONS

Ts = Saturation Pressure, Kelvin
P = Pressure, kPa
ρl = liquid density, kg / m3
ρg = gas density, kg / m3
hf = liquid enthalpy, kJ / kg
hg = enthalpy vapor, kJ / kg
h = enthalphy fluid, kJ / kg
μ¬l = liquid viscosity, kg / m.s.
μg = viscosity of steam, kg / m.s.
σL = surface tension, N / m
X = Dryness, fraction
Nlv = liquid velocity number
N fr = Froude Number
λ = homogeneous Liquid Holdup
Vs = superficial velocity of water, m / s
Vsg = superficial velocity of water vapor, m / s

Vm = two phase fluid velocity,

W = mass flow rate of water and steam fluids, kg/s

Hl = liquid holdup

Hl (0) = horizontal liquid holdup

C = inclination factor

ftp = friction factor for two phase flow

Nre = Reynould's number.

REFERENCE

Ashat, A.M. 1997. "Making a simulator for Calculation of Pressure Loss on Two-Phase Geothermal Flow Pipes." Bachelor's Final Project. Bandung: ITB Petroleum Engineering Department.

BJ / Leonard, R., 2007. "Solubility Test of Scale Sample From TM 1-5 Well. April 17, 2007, BJ Laboratory Report S-028-04-07-Chevron-TM 1-5-Sol.

BJ / Royce, T., 2007. "Solubility Test of Scale Sample From TM 1-5 Well." BJ Laboratory Report S-020-03-07-Chevron-TM 1-5-Sol dated March 28, 2007

Ejiogu, G.C and M. Fiori. 1987. "High-Pressure Saturated-Steam Correlations". SPE Annual Technical Conference. New Orleans.

Miryani, N. 2008. "Dictate of Geothermal Engineering Lecture". Bandung: ITB Petroleum Engineering Department.

Proceedings World Geothermal Congress 2005 Antalya, Turkey, 24-29 April 2005. "Cerro Prieto Geothermal Field Review of Corrosion and Scaling Problems over 31 Years of Commercial Operations"

Siega, Farrel.L, Edwin B. Herras and Balbino C. Buning. 2005. "Calcite Scale Inhibition: The Case of Mahanagdong Wells in Leyte geothermal Production Field, Philippines." World Geothermal Congress. Makati City: PNOC-Energy development Corporation.

Soendaroe, Achmad. 1997. "Forecasting the Performance of Large-Diameter Geothermal Wells". Bachelor's Final Project. Bandung: ITB Petroleum Engineering Department.

Syufyan, Hidayatus. 2009. "scaling problem in AWI 1-5 geothermal well". Job Training Report. Bandung: ITB Petroleum Engineering Department.

Tassew, Merga. 2001. "Effect of Solid Deposition on Geothermal Utilization and Methods of Control". Geothermal Training Program. Ethiopia: Ethiopian Elektric Power Corporation.

Tortike, W.S. and Farouq Ali S.M. 1989. "Saturated-Steam-Property Functional Correlations for Fully Implicit Thermal Reservoir Simulation." SPE Publication. University of Alberta.

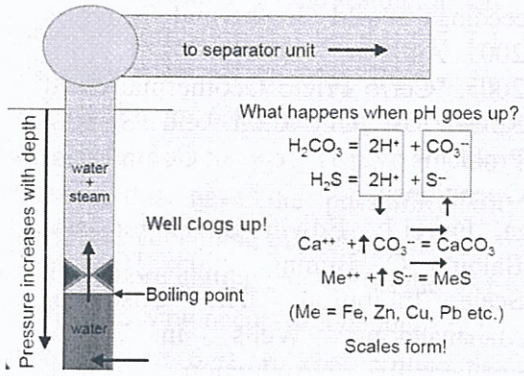

Figure 2.1. Scaling of geothermal wells[4)]

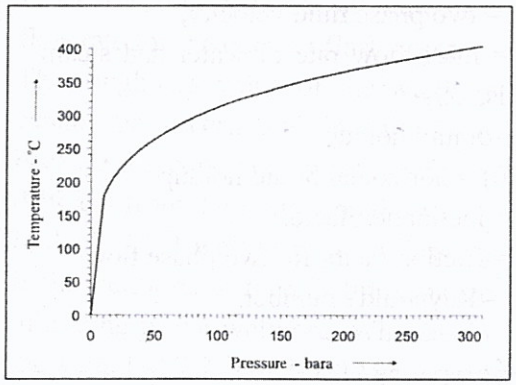

Figure 3.1 Saturation Temperature as a Pressure Function[3)]

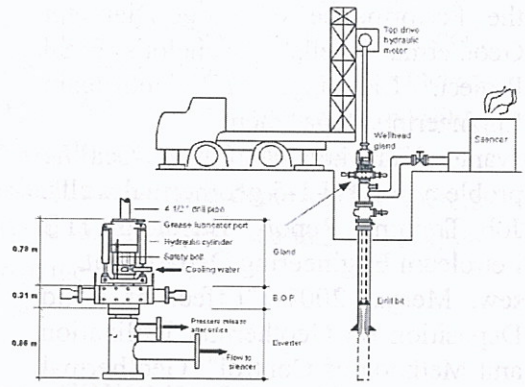

Figure 2.2. Drillbit and Scraper Tools[11)]

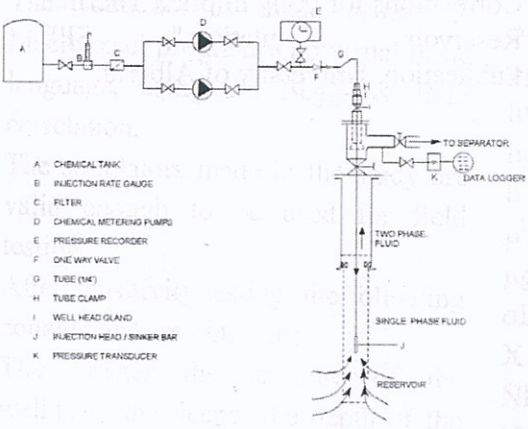

Figure 2.3. Chemical Scale Inhibitor [11)]

Lajur Alir Massa	:	27.5	kg/s
WHP/BHP	:	4.5	bara
Enthalpy	:	1500	Kj/Kg
Temperature	:	250	Celcius
Depth increase	:	100	meter
Kedalaman casing	:	502	meter
Diameter casing	:	13.375	in
Diameter Liner	:	9.625	in
Kedalaman Liner	:	840	meter
Diameter perf Liner	:	7	in
Kedalaman perf Liner	:	1164	meter

RUN

CLEAR

Kelarutan Amorf	:	0.76	
Kelarutan Quartz	:	1.03	
Densitas Silika	:	43.442	g/in3

Figure 5.1 Input Simulator Data

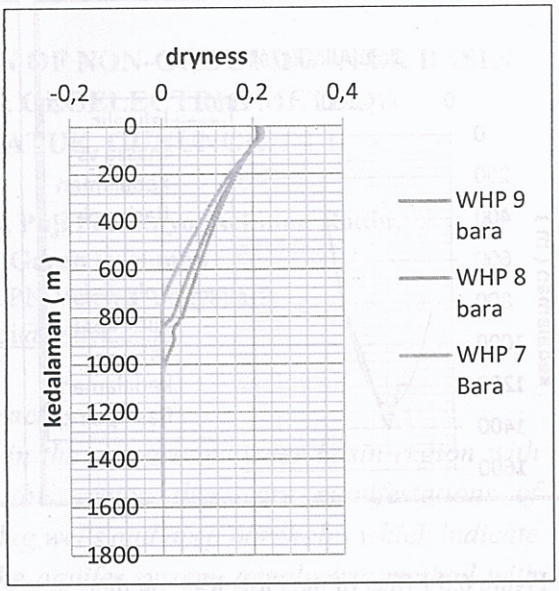

Figure 6.1 Effect of the Pressure of the Well Head on the Flash Point Depth.

Data keluaran

Kedalaman (m)	Tekanan (bara)	Temp (celsius)	pola aliran	fraksi uap	Laju Penebalan Silika (inch/tahun)
0	4.5	155.344	segregated	0.402768895	2.41661337265
100	6.5101661	155.343	segregated	0.402770343	2.41662205912
200	8.5203321	167.7155	segregated	0.384513912	2.30708346957
300	10.530498	177.7006	segregated	0.369269632	2.21561779228
400	12.540664	186.1469	segregated	0.355964073	2.13578443690
500	14.55083	193.5093	segregated	0.34402401	2.06414406204
600	16.560996	203.4638	segregated	0.327321193	1.96392715644
609.625	16.813266	203.4637	segregated	0.32732124	1.96392743837
619.25	17.065535	204.1977	segregated	0.326062606	1.95637563745
628.875	17.317804	204.9232	segregated	0.324814679	1.94888807425
638.5	17.570074	205.6404	segregated	0.323577181	1.94146308811
648.125	17.822343	206.3496	segregated	0.322349848	1.93409908505
657.75	18.074612	207.051	segregated	0.321132422	1.92679453417
667.375	18.326882	207.7447	segregated	0.319924661	1.91954796424
677	18.579151	208.431	segregated	0.318726327	1.91235796055
686.625	18.83142	209.11	segregated	0.317537194	1.90522316197
696.25	19.08369	209.782	segregated	0.316357043	1.89814225815
705.875	19.335959	210.447	segregated	0.315185664	1.89111398698
715.5	19.588228	211.1053	segregated	0.314022855	1.88413713213
725.125	19.840498	211.7569	segregated	0.31286842	1.87721052080
734.75	20.092767	212.4021	segregated	0.31172217	1.87033302161
744.375	20.345036	213.041	segregated	0.310583924	1.86350354254
754	20.597306	213.6738	segregated	0.309453505	1.85672102912
763.625	20.849575	214.3005	segregated	0.308330744	1.84998446261
773.25	21.101844	214.9213	segregated	0.307215476	1.84329285835
782.875	21.354114	215.5363	segregated	0.306107544	1.83664526421

Figure 5.2 Example of Simulator Output Data

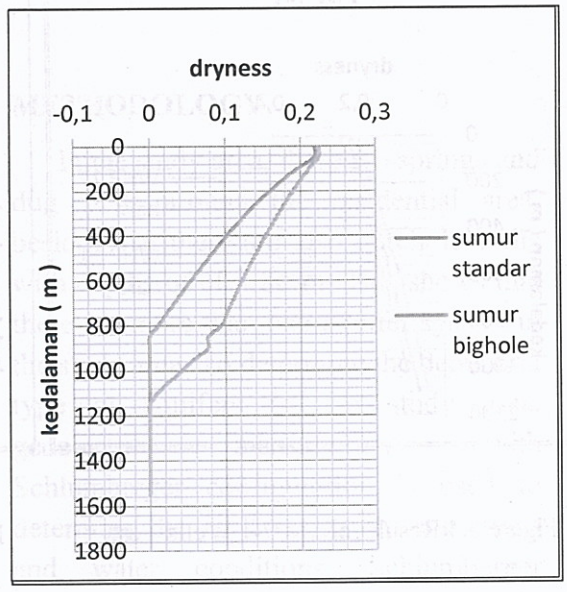

Figure 6.2 Effect of Combination of Well Size Types on Flash Point Depth.

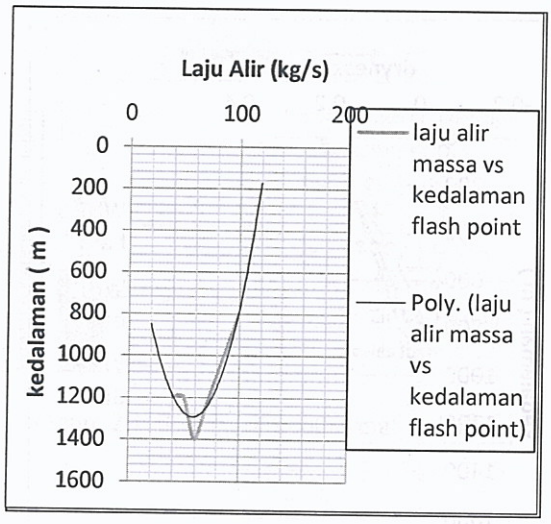

Figure 6.3 Effect of the Flow Rate on the Flash Point Depth.

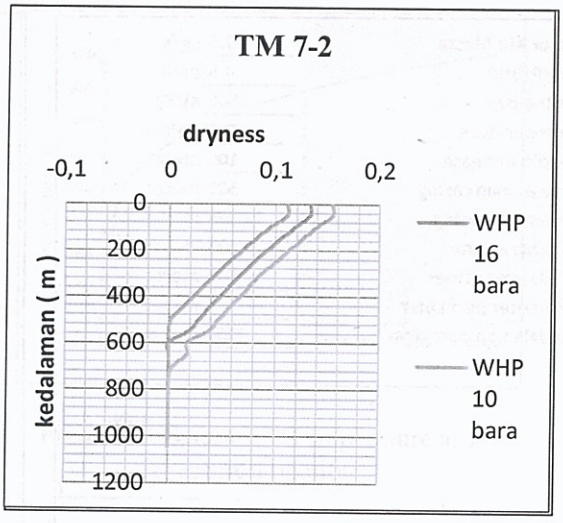

Figure 6.5 TM 7-2 Wells Test Results.

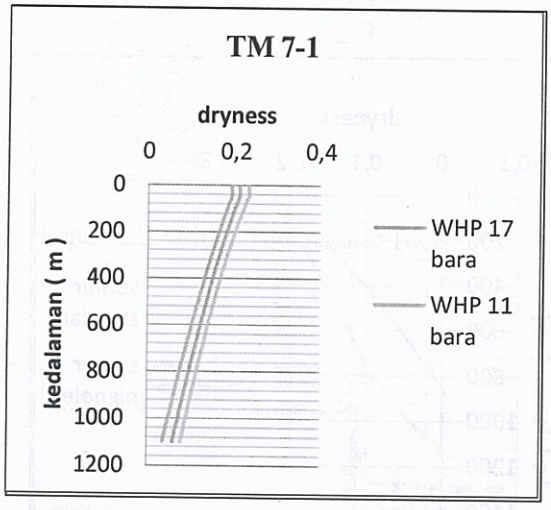

Figure 6.4 Results of TM 7-1 Wells Test.

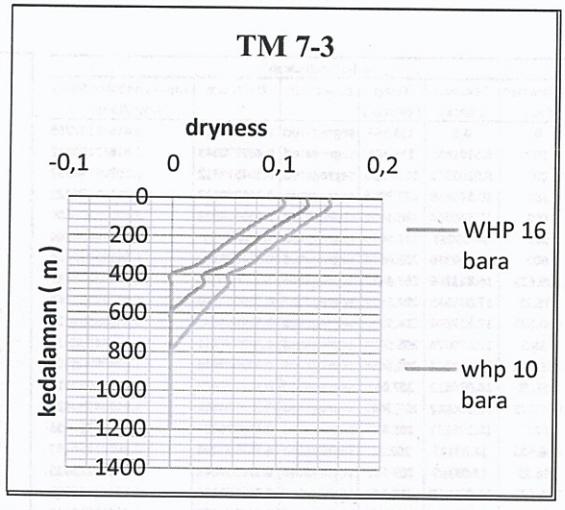

Figure 6.6 Test Results of TM 7-3 Wells.